A. Kinney
SIB

FOS Blue Detector Plate Scale and Orientation

Anuradha Koratkar
Space Telescope Science Institute
Instrument Science Report CAL/FOS-087

ABSTRACT

Inflight plate scale factors for the FOS blue detector are measured for the first time from the cycle 1 proposal ID number 3366 data. The analysis indicates that the scale factors are 1.48"±0.03" per diode height and 0.368"±0.01" per diode width. The uncertainity in the analysis due to GIMP correction is of the same order as the difference in the plate scale calculated from the present analysis and the prelaunch specifications. Hence, the present prelaunch plate scale factors of 1.43" perdiode height and 0.357" per diode width need not be changed in the database.

A mean rotation angle of $-0.12°\pm0.37°$ is measured between the FOS Y axis and the direction perpendicular to the diode array. Similarly, a mean rotation angle of $-2.03°\pm0.36°$ is measured between the FOS X axis and the direction parallel to the diode array. These negligiblely small rotation angles indicate that the orientation of the diode array is well aligned with the FOS XY axes.

1.OBSERVATIONS AND ANALYSIS

The star GRW +70D5824 was observed on day 53 of 1992 to determine the precise plate scale of the FOS blue detector. The observations were in the image mode through the 4.3 arcsecond aperture and with the camera mirror. The high voltage for these observations was 22.84 kilovolt. Two sets of 5×3 step and dwell scans were performed. The step sizes were 1" or 2" along the diode array (X-direction) and 1" perpendicular to the array (Y-direction). The scan pattern is shown in Figure 1. Each image had 4 sub-steps per diode width and 16 Y-steps. Hence, each image has 744×16 pixels. In 12 of the 30 observations (positions are denoted by * in Figure 1) the star was too near the edge of the aperture and the stellar image center could not be precisely measured. Further, these 12 observations could also be affected by vignetting due to the proximity of the star to the aperture edge. Hence, these 12 points are not included in the analysis. In Figure 1, the positions of the excluded observations have been roughly calculated from the other 18 well determined positions to show the scan pattern.

The STSDAS tool APERLOCY is used to determine the stellar image center in mea-

sured FOS instrumental units. The three methods used to locate the center are, 1) geometric midpoint, 2) flux centroid and 3) cross correlation using a boxcar template. In the cross correlation technique, a 5×5 cross correlation template is used to locate the aperture center. This template size is considered to be adequate since the aperture is not uniformly exposed. The centers determined by the flux centroid and the cross correlation technique are consistent within the measurement errors. The image centers determined by the cross correlation technique are used in the following analysis. The coordinates of the image center are not corrected for geo-magnetically induced image motion (GIMP) in the Digicon detector, because the effect of GIMP on the blueside is small, and in the image mode due to frequent de-perming of the digicon the effect is further reduced. The X and Y coordinates of each image center are given in Table 1.

The relative X and Y position in FGS encoder units for each observation was also calculated from the FGS encoder values by determining the centroid of the jitter at each dwell point during the observation (Fitch and Lupie Private communication). Next the FGS offsets (in arcsec on the sky) in the X and Y direction in the two raster scans were calculated from the FGS astrometric calibration (Fitch and Lupie Private communication), and compared with the commanded offsets (see columns 2 and 3 of Table 2). Table 2 shows that an average Y–offset of 1.0004±0.004" is executed when the telescope is commanded to offset 1". The step sizes are accurate to within 0.4% (or about 4 mas) in the Y-direction. The average offset executed in the X-direction was 1.9981±0.005" when commanded to offset 2", and 0.9966±0.003 when commanded to offset 1". The step sizes are accurate to within 0.3% (or about 4 mas) in the X-direction.

The offsets determined by using APERLOCY (see columns 4 Table 2) indicate that, in the Y–direction an average 173.1979±3.993 y–base shift is seen when the telescope is commanded to offset 1.0003". Similarly, in the X–direction an average 2.7385±0.057 diodes shift is seen when commanded to offset 0.9966", and 5.3587±0.0276 when commanded to offset 1.9981".

2. RESULTS

Binary target acquisition constraints require the effective diode height to correspond to 256 y–base units. This analysis indicates that a 1" offset produces an average shift of 173.146 y–base units (see Table 2a). Hence, the effective diode height is 1.48" instead of the pre-launch value of 1.43". The difference in the effective diode height, calculated from the present analysis and the prelaunch specifications, is −2.8%±2.3%. This difference is 4.75μm using a conversion factor of 0.8086μm per y–base unit. Since the diode response at the ends is not perfectly sharp and is affected by the conductors at the ends, the deviation in the effective diode height from the prelaunch specification is reasonable.

In the X-direction (along the diode array) this analysis indicates that a 1" offset produces an average shift of 2.7148 diodes (see Table 2b). The pre-launch scale factor indicated that a 1" offset should produce a shift of 2.801 diodes. The difference, calculated from the present analysis and the prelaunch specifications, is 3.1%±2.3%. This is a difference of 1.59μm using a conversion factor of 50μm per diode.

The difference in the platescale calculated from the present analysis and the prelaunch specifications is of the same order as the measurement error in the analysis. This measurement error in the analysis is due to the small but unknown GIMP correction. Hence, it is recommended that the prelaunch platescale values in the database not be changed.

The 18 observations used in the analysis form 6 roughly straight lines in the X-direction (along the diode array) and 6 lines in the Y-direction (perpendicular to the diode array). See Figure 1. The orientation of the diode array with respect to the FOS XY coordinate axes is calculated by determining the slopes of these 12 lines. The 12 lines in Table 3 are represented by the deflection points in each line. Table 3 also shows the correlation coefficent for the 3 points in each line, the slope of the line formed by the 3 points and the angle of diode array with respect to one of the FOS XY axes. A mean rotation of $-0.12°\pm0.37°$ is measured with respect to the Y-direction, and a mean rotation of $-2.02°\pm0.36°$ with respect to the X-direction. According to the prelaunch specifications the diode array should be perfectly alligned with the FOS XY axes. This analysis shows that the mean rotation of the diode array with respect to the FOS XY axes is neligible. Therefore, there is no deviation in the orientation of the diode array from prelaunch specifications.

3. CONCLUSIONS

The measured plate scale and orientation indicate that the present (pre-launch) values for the blueside diode array are sufficiently accurate. A similar result, i.e., pre-launch plate scale being sufficiently accurate, was obtained for the red detector (Instrument science report FOS/CAL-068, B. Bhatacharya and G. Hartig, Nov 1991). Offset error on the order of 0.06" could be produced over the half-width of the 4.3" aperture due to the changes measured in the plate scale.

Figure 1

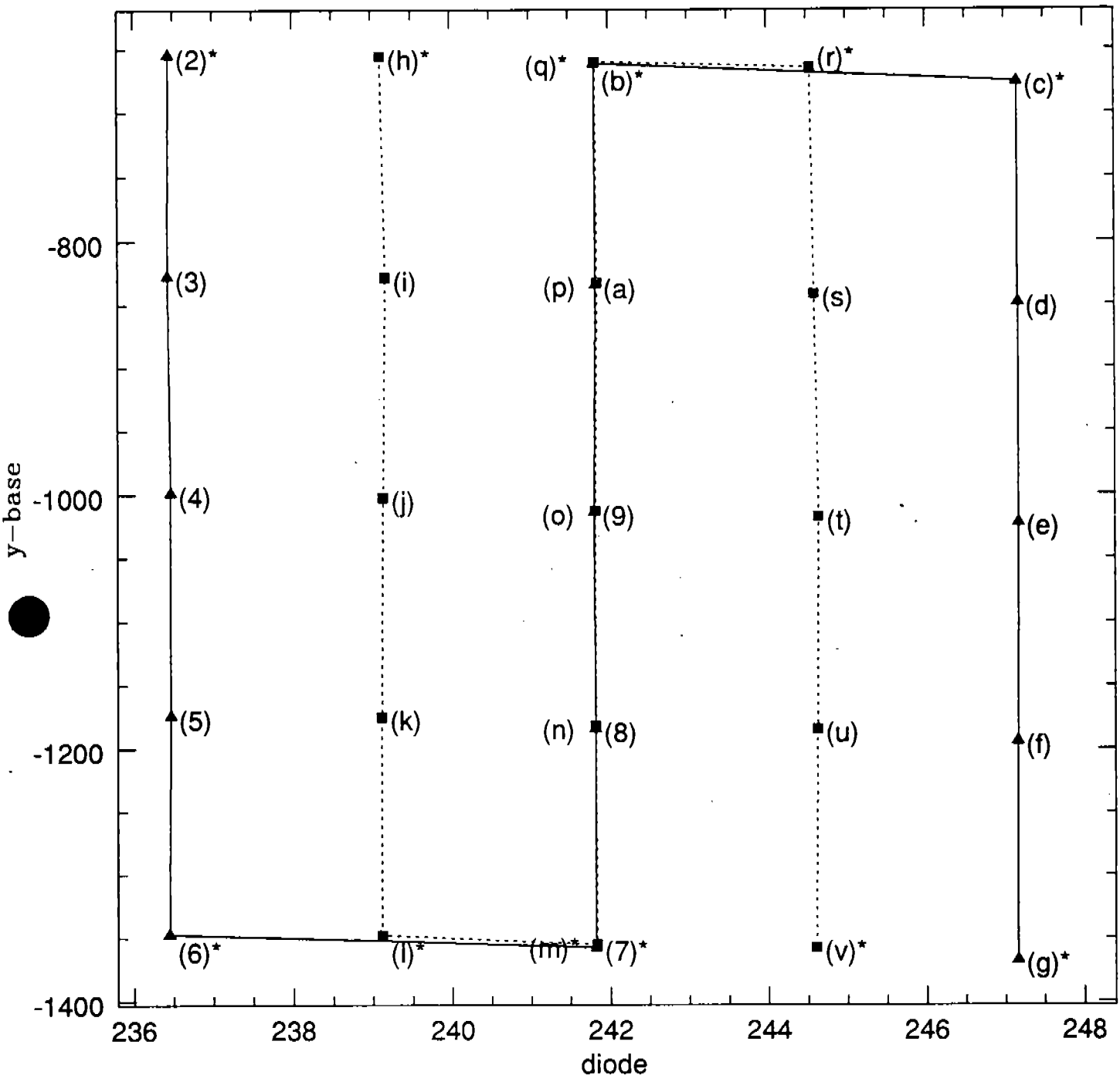

FIG–1. The two scan patterns (solid line with triangles and dotted line with squares) are shown in FOS instrumental coordinates. The 30 observations are identified by the next to last character from the image rootname in Table 1. The 12 observations excluded from the analysis are indicated by *.

Table 1: Stellar Image Centers

Image	X crosscor (diodes)	Y crosscor (y–base)
y0vb0103t	236.4236	−827.5956
y0vb0104t	236.4599	−998.5773
y0vb0105t	236.4613	−1174.0107
y0vb0108t	241.8169	−1184.4270
y0vb0109t	241.8055	−1014.2235
y0vb010at	241.8337	−835.0203
y0vb010dt	247.1686	−849.1306
y0vb010et	247.1719	−1022.4096
y0vb010ft	247.1567	−1194.4243
y0vb010it	239.1708	−828.7468
y0vb010jt	239.1379	−1002.6434
y0vb010kt	239.1114	−1174.9755
y0vb010nt	241.8194	−1182.0972
y0vb010ot	241.8264	−1013.4219
y0vb010pt	241.8506	−833.4568
y0vb010st	244.5918	−842.1360
y0vb010tt	244.6373	−1017.9982
y0vb010ut	244.6222	−1184.5262

Table 2a: Raster Scan Displacements in Y–Direction

Deflection Points	Commanded Shift (arcsec)	FGS Shift (arcsec)	Actual Shift (y–bases)
3–4	1.0	0.9990	170.9817
4–5	1.0	0.9982	175.4334
8–9	1.0	1.0013	170.2035
9–a	1.0	1.0048	179.2032
d–e	1.0	1.0047	173.2790
e–f	1.0	0.9956	172.0147
i–j	1.0	1.0031	173.8966
j–k	1.0	1.0027	172.3321
n–o	1.0	0.9963	168.6753
o–p	1.0	1.0016	179.9651
s–t	1.0	1.0007	175.8622
t–u	1.0	0.9966	166.5280

Table 2b: Raster Scan Displacements in X–Direction

Deflection Points	Commanded Shift (arcsec)	FGS Shift (arcsec)	Actual Shift (diodes)
i–p	1.0	0.9986	2.6798
p–s	1.0	0.9965	2.7412
j–o	1.0	0.9957	2.6885
o–t	1.0	1.0017	2.8109
k–n	1.0	0.9931	2.7080
n–u	1.0	0.9941	2.8028
3–a	2.0	1.9938	5.4101
a–d	2.0	1.9943	5.3349
4–9	2.0	2.0005	5.3456
9–e	2.0	1.9949	5.3660
5–8	2.0	1.9972	5.3556
8–f	2.0	2.0032	5.3398

Table 3: Orientation

Deflection Points	Correlation Coefficient	Slope of Line	Θ
		with respect to the Y-direction	
3–4–5	−0.878	-1.084×10^{-4}	−0.384
8–9–a	−0.604	4.904×10^{-5}	0.174
d–e–f	0.743	3.440×10^{-5}	0.122
i–j–k	0.998	-1.716×10^{-4}	0.608
n–o–p	0.958	8.999×10^{-5}	0.319
s–t–u	−0.668	-9.037×10^{-5}	−0.320
		with respect to the X-direction	
3–a–d	−0.984	−2.003	−1.855
4–9–e	−0.984	−2.224	−2.060
5–8–f	−1.000	−1.909	−1.768
i–p–s	−0.987	−2.473	−2.290
j–o–t	−0.971	−2.783	−2.577
k–n–u	−0.959	−1.728	−1.601